Comparison between Binder and Hot Mix Asphalt Properties and Early Top-Down Wheel Path Cracking in a Northern Ontario Pavement Trial

Thomas Bodley,[1] Adrian Andriescu,[1] Simon Hesp,[1] and Kai Tam[2]

ABSTRACT

The primary objective of this paper is to evaluate the usefulness of various asphalt binder and mixture properties for predicting field performance in terms of top-down fatigue cracking. A secondary goal is to discuss how various modification technologies for obtaining a given Superpave® grade can lead to significant differences in service performance.

Different binder and mixture tests were evaluated in an attempt to explain early top-down wheel path cracking in three of seven test sections of a pavement trial on Highway 655 north of Timmins, Ontario. The trial was constructed in the summer of 2003 with 500 m long, side-by-side sections that contained a variety of modified binders: five of PG 64-34, one of PG 58-34, and a control section of PG 52-34. Modification additives and technologies employed included reactive ethylene terpolymer (RET), polyphosphoric acid or phosphoric acid (PPA and H_3PO_4), oxidation, styrene-butadiene-styrene (SBS), and combinations thereof.

The test sections were exposed to record low temperatures during January 2004 when the temperature at 5 mm below the pavement surface reached –34ºC on two occasions. A visit in late January 2004 showed little distress except for minor transverse cracking in transition areas. In contrast, a detailed survey in late April 2004 revealed that by then three test sections had cracked severely, with a total of approximately 143 m of wheel path cracks and several pronounced transverse cracks. Nearly all load induced cracking was confined to the inside of the left wheel path in the

[1] Department of Chemistry, Queen's University, Kingston, Ontario K7L 3N6.
[2] Bituminous Section, Materials Engineering and Research Office, Ministry of Transportation of Ontario, Downsview, Ontario M3M 1J8.
The oral presentation was made by Mr. Bodley.

southbound lane, in a location which is subjected to the highest combination of traffic and thermal stresses. In early July 2006 the total longitudinal cracking in the three affected test sections had increased to over 300 m while several wheel path cracks as well as the centreline joint had started to initiate transverse cracks. The four other test sections have remained largely free of cracks.

Asphalt binders and mixtures were tested by using various approaches. Binder tests included: (1) Superpave® grading; (2) dynamic shear and bending beam rheometer testing to determine rheological master curves, Black space diagrams, and low temperature grade losses due to reversible aging processes during extended conditioning; (3) penetration-viscosity grading; and (4) double-edge-notched tension testing to determine master curves of ductile failure properties. Mixtures were tested using the following methods: (1) dynamic compression to determine the complex modulus and phase angle master curves; (2) dynamic fatigue in four-point bending; (3) dynamic creep fracture in compact tension; and (4) monotonic rate tests on double-edge-notched tension specimens to determine essential and plastic works of fracture, as well as approximate critical crack tip opening displacements.

An analysis of the findings suggests that only the monotonic double-edge-notched tension test results correlated reasonably well with field distress. It was found that the ductile failure data needed to be supplemented with reversible aging tendencies to provide a complete interpretation of the distress variation experienced within the trial.

Key Words: Hot Mix Asphalt, Top-Down Cracking, Thermal Cracking, Field Validation, Polymer Modification, and Acid Modification

INTRODUCTION

This paper documents and discusses the investigation of various asphalt binder and mixture tests to predict wheel path fatigue cracking in the field. Although a number of publications have proposed various ways of obtaining parameters that are considered useful for the ranking of asphalt in terms of fatigue resistance, a consensus on which method is most desirable has yet to be found. An ideal test should provide an accurate, simple, and reproducible property that is consistently able to rank performance in well-controlled trials and in practice. It would be most convenient if this test were one for the asphalt binder or mastic, since that would significantly reduce sample preparation time and equipment costs. It would also be desirable if the test could be done in monotonic loading rather than cyclic loading, which would involve more complex equipment and advanced data analysis protocols. If no single test (property) is able to fulfill these requirements, then a set of tests (properties) may need to be considered to address the issue of performance grading for fatigue.

The work described herein forms part of an effort to develop improved asphalt specification test methods, criteria, and associated limits for such criteria. Significant progress has been made in recent years with the development of an extended bending beam rheometer (BBR) test, use of which should significantly reduce transverse cracking distress in years to come (*1*). Once fewer low temperature cracks appear, the next logical step would be to better control fatigue failure. To this end a significant amount of work has been done to develop a new asphalt binder and mixture testing approach that measures failure properties in the high strain regime (*2-5*). This work is supported through the Ontario Ministry of Transportation, which has recently constructed two pavement trials on Highways 655 (Timmins) and 417 (Ottawa), respectively, and has approved a third trial for Highway 655 to be constructed in 2007. Once completed, this construction effort will provide a total of 22 test sections approximately 11 km in length made with a wide variety of modified and straight binders. Ontario has recently published the extended BBR protocol (*1*) as well as a draft version of the double-edge-notched tension (DENT) test (*5*). It is hoped that transverse and wheel path cracks will be better suppressed once these methods are implemented.

The objective of this paper is to correlate various binder and mixture test results with the recently obtained wheel path fatigue data from the first Highway 655 trial (*6*). Since all sections were modified with various technologies, a short discussion on the potential merits of various additives is also included.

BACKGROUND

Fatigue Grading

A detailed discussion of various fatigue grading approaches is given in a previous paper discussing the FHWA ALF (*4*) and in Andriescu, 2006 (*7*). Hence, only an abbreviated review is provided here to place the current work in context.

The early work on fatigue testing of asphalt binders and mixtures focused on purely phenomenological relationships between induced load or displacement level and cycles to failure (*8*). The fatigue life can be expressed in the form of a power law with various fitting constants that reflect the sensitivity to initial strain (or stress) and stiffness (*9*). The validity of such a relationship is limited for different designs and asphalt sources. It is therefore useful to consider a more fundamental performance ranking of asphalt binders and mixtures.

A more rational approach to fracture, based on the concept of dissipated energy, was proposed by Van Dijk in 1975 (*10*). The effort by Van Dijk served to prove that force and displacement controlled tests lead to the same result (*10*, *11*). Experiments done as part of the SHRP program confirmed Van Dijk's 1975 findings but showed that fatigue life and cumulative dissipated energy are still mix and temperature dependent, making the practical use of this relation difficult (*9*).

More recent studies by Aglan and co-workers (e.g., (*12*)), Kim and co-workers (e.g., (*13, 14*)), Lundström and Isacsson (*15*), Uzan et al. (*16*), Roque and co-workers (e.g., (*17-20*)), and many others focus on separating the damage energies from the non-essential energies in the failure process.

A rather simple approach to separate the energies involved in the fracture process zone from those involved in viscous and plastic dissipation away from the crack zone was developed at

Queen's University based on the essential work of fracture (EWF) analysis (*2-5*), as first applied to metals and plastics by Cotterell and Reddel in 1977 (*21*) and further developed by Mai and co-workers (*22*). The EWF approach is based on a separation of the essential work of fracture, w_e, absorbed in the fracture process zone, from the plastic work of fracture, w_p, or non-essential energy, dissipated away from the fracture process zone.

Cotterell and Reddel (*21*) were the first to propose that w_e scales with the ligament length times the sample thickness, $L \times B$, and that the w_p term is proportional to the plastic zone size, which can be approximated as elliptical, circular, or diamond shaped, and hence scales with the square of the ligament length, L^2. In mathematical form the specific total work of fracture, w_t, is divided into two parts:

$$w_t = W_t/LB = (w_e\, LB + \beta w_p L^2 B)/LB = w_e + \beta w_p L \qquad (1)$$

where W_t is the total work of fracture in a DENT test as provided by the area under the force-displacement curve (J), L is the ligament length (m), B is the sample thickness (m), β is a geometrical constant which depends on the shape of the plastic zone, w_e is the specific essential work of fracture (J m^{-2}), and w_p is the specific plastic work of fracture (J m^{-3}) (*7*).

Equation 1 shows that when the specific total work of fracture is plotted versus the ligament length, a straight line should be obtained with intercept w_e and slope βw_p. This has been confirmed for a large number of straight and modified asphalt binders and mixtures (*2-4, 7*).

Further, it was found that the critical crack opening displacement, as approximated by the essential work of fracture divided by the net section stress in the smallest ligament specimen, $\delta_t = w_e/\sigma_{n,\,5\ mm}$, provided an improved correlation with fatigue cracking severity in the FHWA ALF sections over that of the binder loss modulus, $G^*\sin\delta$ (*4*). The δ_t parameter provides a measure of strain tolerance in the ductile state and in the presence of a high degree of stress concentration. Hence, it shows promise for performance grading of both binders and mixtures for fatigue cracking at temperatures and rates of loading that cover the ductile regime.

Top-Down Cracking

While the problem of top-down cracking has been reported in the literature for a long time, it has recently gained more attention as an active topic of research in both North America and Europe (*18, 20, 23-25*). For a detailed review of the causes and mechanisms of top-down cracking, the reader is referred to these prior publications. The main factors of importance are thought to include surface hardening, weak or stiff subgrades combined with temperature profiles that produce high stiffness gradients within the pavement, high tensile stresses at the edges of truck tires or in between truck tires, low fracture energies, segregation during construction, and other less understood issues.

It is likely that there is no single property or test that can predict the level of top-down cracking when it occurs to varying degrees due to more than one mechanism at various temperatures and rates of loading. However, this paper presents some unique results suggesting that for thin pavements the reversible aging tendency of the binder, as determined by the extended BBR test method LS-308 (*1*), and the critical crack opening displacement (CTOD or δ_t), as measured with the DENT test method LS-299 (*5*), could provide promising tools for the elimination of top-down cracking in early life and could prevent premature failures as seen in several contracts (*3, 26*). It will also be discussed why essential and plastic works of fracture (w_e and w_p) may need to be considered to control fatigue distress in properly designed long-life pavements.

EXPERIMENTAL

Highway 655 Pavement Trial

The Highway 655 trial is located some 60 km north of Timmins, Ontario, and was constructed during the summer of 2003. All seven sections are 500 m in length, cover both lanes, and were placed in two lifts for a total of 90 mm hot mix asphalt on new granular material. Each test section comprised a 50 m transition area followed by a 100 m sampling area, 200 m monitoring portion, and another 150 m sampling area. Since the

age of the trial was only several months at the time of the first distress survey, and since no significant coring had taken place, we report herein the cracking distress that was observed within each 500 m section. The few cracks that appeared very close to the transition joints or around QCQA cores are not considered in the discussion.

Thermocouples were embedded within the pavement in two locations approximately 5 mm below the surface in between the wheel paths. Each location had a logger with four separate thermocouple wires (type T) that were buried in the subgrade and glued in place after construction at the desired depth below the surface. Temperatures were recorded at 30 minute intervals. One of the loggers failed during the spring of 2004 when water flooded the box in which it had been buried, while the second logger failed in a similar manner during the third winter. However, accurate pavement temperature readings were obtained for the first two years, while accurate air temperature readings were obtained for all three years from two loggers that were positioned in trees on either side of the road. Pavement temperatures agreed remarkably well using the LTPPBind® algorithm (*27*). Hence, it was decided that air temperatures will suffice in years to come.

The site has been visited each of the last three years. Cracks were surveyed in detail on January 30 and April 24, 2004, with a more cursory survey conducted in early 2005. In early July 2006 an additional comprehensive survey was done. During July 2005 a detailed falling weight deflectometer (FWD) and soils investigation was conducted (*28*), the results of which will be discussed in relation to the cracking distress.

Materials

The materials in this study were obtained in sufficient quantities from the sampling spigot of the asphalt line feeding into the asphalt plant and from the various stockpiles of aggregate adjacent to the plant. Binders were stored in sealed containers until used, and aggregates were dried overnight prior to their use for specimen preparation.

A detailed description of the standard binder properties as determined by various laboratories is provided in tables 1-3.

TABLE 1. Superpave® Properties

Binder	Modification Type	Grade, ºC	G*sinδ @ 16ºC, kPa	$T_{G^*\sin\delta = 5\ MPa}$, ºC
1	RET + PPA	65-36	2218	9.8
2	Ox + SBS	65-36	2588	10.1
3	SBS	65-36	1954	7.8
4	SBS + P[31]	67-35	2226	9.1
5	SBS	66-35	2273	9.7
6	Ox + P[31]	59-35	1820	7.1
7	P[31]	54-35	1542	6.7

Note: RET = reactive ethylene terpolymer; PPA = polyphosphoric acid; Ox = oxidized; SBS = styrene-butadiene-styrene; P[31] = additive containing phosphorous. Continuous grades are rounded to the nearest degree, are averages from three laboratories, and varied by less than 1.9ºC between laboratories.

TABLE 2. Viscosity and Penetration Values

Binder	Viscosity @ 60ºC, Pa.s	Pen @ 25ºC, dmm (100 g, 5 s)	Pen @ 4ºC, dmm (100 g, 5 s)
1	369	151	18
2	217	125	17
3	521	147	23
4	1618	124	18
5	2600	128	19
6	204	128	20
7	47	235	24

TABLE 3. Limiting BBR Grading Temperatures of Unaged, RTFO, and PAV Residues and RTFO Mass Losses

Binder	Unaged	RTFO mass change, %	RTFO-aged	PAV-aged
1	-37.7	-0.57	-36.7	-35.7
2	-40.9	-0.51	-39.3	-35.7
3	-42.0	-0.55	-40.9	-37.0
4	-41.0	-0.28	-40.3	-36.0
5	-38.9	-0.46	-37.7	-35.4
6	-40.2	-0.25	-39.3	-34.6
7	-40.8	-0.42	-39.7	-34.7

Note: All grades were obtained at Queen's University hence PAV numbers differ slightly from those listed in table 1.

The surface course mix was used for all experiments in this study. It consisted of a Superpave® 12.5 mm design with an optimum asphalt binder content of 5.2 percent. The mixture contained coarse aggregate and screenings fractions of hard volcanic rock and a natural sand fraction from a local river source.

Procedures

Binder Preparation and Testing

The binder properties as listed in table 1 were determined according to standard procedures on unaged, rolling thin film oven aged (RTFO), and pressure aging vessel aged (PAV) residues at Queen's University, the Ontario Ministry of Transportation, Imperial Oil, and by the Contractor. The properties listed in table 2 were all determined at Imperial Oil in Sarnia, Ontario. The limiting BBR grades listed in table 3 were determined at Queen's University. The effects of low temperature conditioning on the grade temperature was studied according to a new Ontario test method, *LS-308 – Method of Test for Determination of Performance Grade of Physically Aged Asphalt Cement Using Extended Bending Beam Rheometer (BBR) Method* (*1*).

A dynamic shear rheometer (Rheometrics RDA-II) was used to determine rheological properties (G*, G', G'', tanδ, shift factors, etc) for all binders over a wide range of temperatures. Some of the master curves are presented in the discussion section of this paper.

The essential work of fracture tests on binders were conducted on an MTS Sintech 2/G test frame. The procedure is now described in a new Ontario test method, *LS-299 (Draft) – Method of Test for Asphalt Cement's Resistance to Fatigue Fracture Using Double-Edge-Notched Tension Test (DENT)* (*5*), while additional details can be found in earlier publications (*2-4*). In brief, DENT samples were poured in silicone molds in which aluminium inserts were placed for attachment to the load frame. Ligament lengths varied from 5 mm to 25 mm (L) in a 30 mm wide (W) and 6.5 mm thick (B) specimen. Tests were conducted after conditioning at the test temperature for approximately 24 hours. Loading rates varied from a low of 0.1 mm/min to a high of 3,000 mm/min at temperatures from –12ºC to +36ºC. The results of these tests were used to determine the master curves of the ductile failure properties w_e and βw_p. Shifting was done to a reference temperature of 0ºC. The

comparison between shift factors from DSR and EWF is discussed in Andriescu (*7*).

Mixture Preparation and Testing

In this study only the surface mixture with a maximum aggregate size of 12.5 mm was evaluated. Aggregates and asphalt binder were blended in the laboratory using a bucket mixer. Loose mix was short term oven aged at 150ºC for two hours prior to compaction. Both gyratory and slab compactors were used to prepare specimens. Gyratory specimens prepared were 15 cm in diameter and approximately 18 cm in height. Slabs were 60 cm in length by 40 cm in width and either 10 cm or 13 cm in thickness.

Void contents were determined after cutting by weighing dry, wet/surface dry, and under water. Most samples tested had voids within a 2 percent range around the average. All mixture numbers in this paper correspond to section numbers in the trial (i.e., mixture 1 was made with identical materials and composition as those for section 1).

A simple performance tester (SPT) manufactured by IPC Global was utilized for determining the complex modulus and phase angle master curves. Cylindrical SPT specimens were cored from laboratory compacted slabs. The cylindrical specimens were 100 mm in diameter and sawed at both ends to 150 mm in height with smooth and parallel cut faces as described in the AASHTO Provisional Standard for Dynamic Modulus Testing, TP62-03 (*29, 30*), and protocol from the Simple Performance Tester for Superpave® Mix Design (*31*). The ends of the specimen were no closer than 25 mm from the compacted slab face, which exceeded the protocol of trimming a minimum of 7.5 mm from each end of a gyratory specimen to ideally achieve uniform air void distribution. Three axial LVDTs were mounted for dynamic modulus testing at 120^{o} apart on studs having a gauge length of 75 mm attached to the sides of the SPT specimen with epoxy, as shown in figure 1 (a).

Prior to SPT testing, the SPT specimens were placed in an environmental chamber to stabilize their temperature with the testing temperature. After the SPT specimen reached equilibrium temperature, two Teflon pads were used on top and beneath the SPT specimen to reduce friction for dynamic modulus testing.

The SPT dynamic modulus tests deviated slightly from established procedures (*29-31*) at a sweep of temperatures of 4, 12,

24, and 36ºC and at frequencies of 10, 1, 0.1, and 0.02 Hz. Nevertheless, sufficient dynamic modulus data were acquired to obtain overlap at different temperatures for master curves of interest. Two specimens with three LVDT's were tested and yielded similar estimated limits of accuracy when using 2 LVDT's and 4 replicates: 13.1% and 13.4%, respectively (*29-31*). Before applying the dynamic load to the specimen, a contact load was applied that was equal to 5 percent of the dynamic load. After that, a compressive haversine dynamic load was applied to the specimen and dynamically controlled by the SPT so that the resulted axial strain was in the range of 75 to 125 μm/m (this varies from mixture to mixture depending on the stiffness and temperature). Following pre-programmed protocols, trial dynamic loads were applied for 10 pre-loading cycles to determine the stress required to maintain 75-125 μm/m dynamic strains, followed by 10 formal cycles to measure the dynamic modulus and phase angle. Details of data reduction and sinusoidal fitting for phase angle and dynamic modulus calculation can be found in Bonaquist et al. (*31*).

(a)  (b) 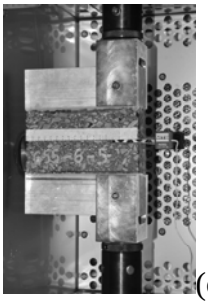 (c) 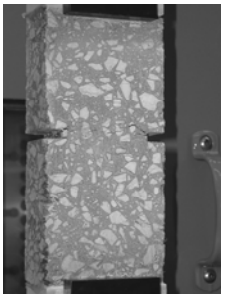

Figure 1. (a) Dynamic Modulus and SPT Sample with LVDT, (b) Dynamic Creep Fracture Test in Compact Tension, and (c) Constant Rate Test in Double-Edge-Notched Tension

Dynamic fatigue in bending was done on an MTS 810 servo-hydraulic test frame. The instrument was equipped with a four-point bending fixture accommodating beams of asphalt concrete 76 mm by 76 mm by 381 mm. Tests were conducted in constant force and constant displacement modes. Repeated haversine pulses of 0.1 s duration were applied without rest periods until the samples failed. All tests were done at room temperature, 25 ± 1ºC. The data were logged with the TestStar IIs software.

The controlled force fatigue data were analysed according to the following failure criteria: (1) a conventional 90 percent reduction in stiffness; (2) a change in the dissipated energy ratio (*32*); (3) a peak in the plot of (stiffness × number of cycles) versus number of cycles (*33*); and (4) a change in the slope of a two-stage Weibull plot (*34*). The controlled displacement fatigue data were analysed according to: (1) a conventional 50 percent reduction in stiffness; (2) a change in the dissipated energy ratio (*32*); (3) a peak in the plot of (stiffness × number of cycles) versus number of cycles (*33*); and (4) a change in the slope of a two-stage Weibull plot (*34*).

It should be noted that the controlled force test measures the resistance to fatigue and creep damage and hence the life measured in such tests may be unrealistically short at a relatively warm test temperature of 25ºC (*35, 36*). Further, the problem associated with the haversine signal in the controlled displacement test relates to the fact that almost instantaneously the force changes into a pure sinusoidal signal while the strain changes into a sinusoidal signal with only about half the displacement of the original haversine pulse (*36*). Hence, both bending tests were not expected to provide a totally representative situation for the way in which the pavement was damaged.

The dynamic creep/fatigue tests on compact tension (CT) specimens were done on an MTS 810 system. Haversine load pulses of 150 N and 0.1 s duration were applied continuously on rectangular specimens of an effective width of 154 mm (W), effective thickness of 40 mm (B), and effective height of 150 mm (H). The initial notch depth was approximately 20 mm (a). Loading was done through aluminium end blocks. Hence, the initial a/W ratio was approximately 0.13. A shallow groove was cut on either side of the specimen to a depth of 5 mm to prevent wandering of the crack. The groove facing the front of the machine was covered with a thin layer of plaster of Paris to facilitate visual observation of crack length. The number of cycles to reach a certain crack length was recorded at 5 mm intervals. The crack growth rate was determined by fitting the raw data to an exponential and then plotting the differential (i.e., smoothed crack growth rate) in a double logarithmic graph according to the Paris law:

$$\frac{da}{dN} = A(\Delta K)^n \quad (2)$$

where a is the crack length (m), N is the number of cycles, ΔK is the stress intensity factor (Pa $m^{0.5}$), and A and n are Paris law constants. The stress intensity factor was determined according to standard equations available elsewhere (*37*). A photograph of a typical CT sample is given in figure 1 (b).

The DENT tests were done on prismatic specimens of approximately 180 mm height (H) by 120 mm wide (W) and 45 mm thickness (B) using an MTS 810 system. A photograph of a typical specimen is given in figure 1 (c). The specimens were glued with high strength epoxy to large aluminium end blocks facilitating homogeneous load transfer. The notch depths varied from 5 mm to 50 mm on either side, giving a ligament length that ranged from 110 mm to 30 mm. Since all tests were done at 25 ± 1ºC, under moderate rates of loading, the displacement was measured with the LVDT attached to the actuator. The specific total works of fracture were determined from the area under the force-displacement curves divided by the cross-sectional area of the ligament, $w_t = W_t/LB$. The essential and plastic works of fracture were determined according to equation 1, while the crack tip opening displacement, δ_t, was approximated by dividing the essential work by the peak net section stress at the smallest ligament, $\delta_t = w_e/\sigma_{net}$. The rate of loading for all specimens was kept constant at 5.4 mm/min (~5×10^{-4} m/m/s). While small changes in the specimen dimensions occurred, these were not considered problematic as they were accounted for based on the fact that the method uses specific works of fracture. For further details the reader is referred to earlier papers (*2-4*).

RESULTS AND DISCUSSION OF RESULTS

Weather Data

Temperature loggers were retrieved from the site in April 2004, April 2005, and June 2006. Figure 2 provides pavement surface temperatures for the first two winters. Useable pavement surface temperatures were obtained from one logger for both 2004 and 2005 while useable air temperature data were obtained from two loggers for all three winters.

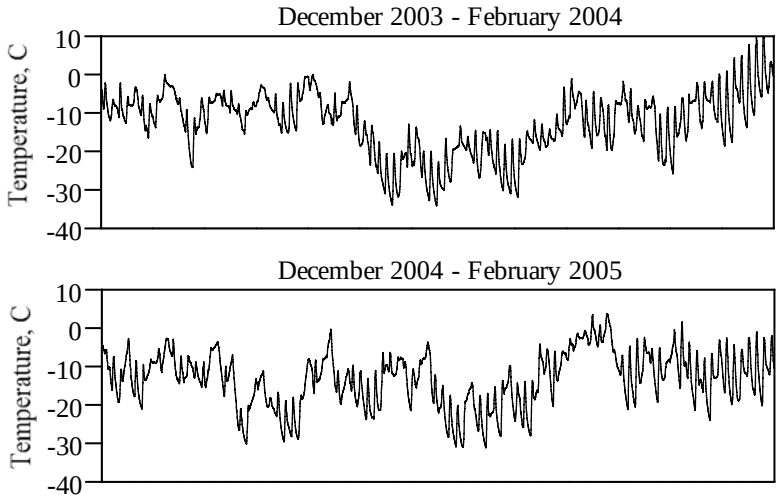

Figure 2. Pavement Surface Temperatures
Note: Pavement temperatures are averaged over four thermocouples. The curves provide temperatures at ~5 mm depth.

The temperatures reached extremes in the first winter with a record low air temperature of around –47ºC on January 9, 2004. The pavement surface temperature (at 5 mm depth) reached –34ºC on two occasions during January 2004 and reached below –30ºC on eight separate occasions. During early 2005 the air temperatures reached around –40ºC on six occasions, while the pavement at 5 mm depth reached below –30ºC on five occasions. In early 2006 the two lowest air temperatures recorded were around –39ºC with what would have been corresponding surface temperatures of around –30ºC or slightly lower.

Hence, this trial is situated in an ideal location for low temperature specification test validation, since temperatures regularly reach close to the design value. The distress observed after the first winter provided us with insight into which factors are of importance for the mitigation of transverse and wheel path cracking.

Cracking Surveys

As mentioned in the experimental section, the cracking distress was surveyed shortly after the severe cold spell of early January 2004 and during the spring thaw in late April 2004. A more cursory survey was conducted in April 2005, followed by a more detailed one in July 2006. Figure 3 shows typical photographs of the wheel path distress found in sections 2, 3, and 4.

Figure 4 shows the cracking severity for all sections in terms of wheel path and transverse cracking for early 2004, while figure 5 shows this for the summer of 2006. It is obvious from the data that for binders of nearly identical grades, there is a considerable variation in terms of distress. Two sections survived the first winter unscathed, while three others were badly damaged. Sections 2, 3, and 4 sustained 60.2 m, 40.1 m, and 43.5 m of wheel path cracking, respectively, making them badly damaged at a very early stage. Section 6 sustained a single wheel path crack of 5.3 m, while section 7 sustained a single transverse crack about half the width of the lane. Sections 1 and 5 survived the first winter unscathed.

From the data in figures 4 and 5 it is evident that the binders in sections 2-4 performed poorly compared to those in sections 1 and 5-7. Section 4 exhibits 50 m of mid-lane cracking, likely due to paver-induced segregation, in addition to the 92 m of wheel path cracks, making it the worst performer.

Most of the longitudinal cracks were located in the southbound lane on the inside of the left wheel path. This is believed to have been because this lane carried loaded logging trucks to Timmins, while they returned empty on the northbound lane. Furthermore, the left wheel path is thought to be under more thermal restraint than the right wheel path, which is closer to the edge of the pavement. Hence, the predominantly triaxial state of stress is thought to have caused the severe distress in this location (*6*). How different factors such as subgrade, construction, and material

properties can also have contributed to the differences between the seven sections is discussed next.

Figure 3. Spring 2006 Wheel Path Cracking in Section 3 (left) and Transverse Crack Initiation in Section 4 (right)

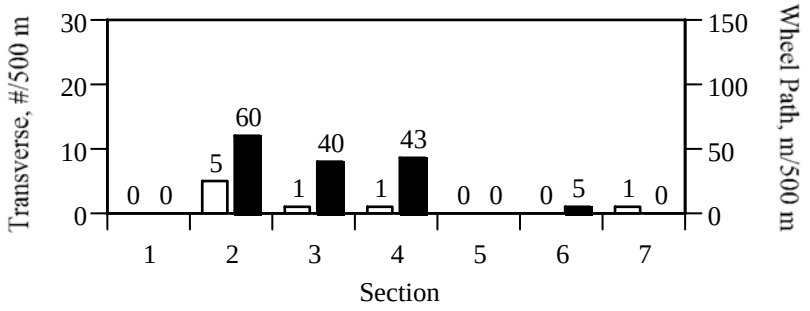

Figure 4. Spring 2004 Crack Survey
Note: Open bars for transverse cracking and solid bars for wheel path cracking.

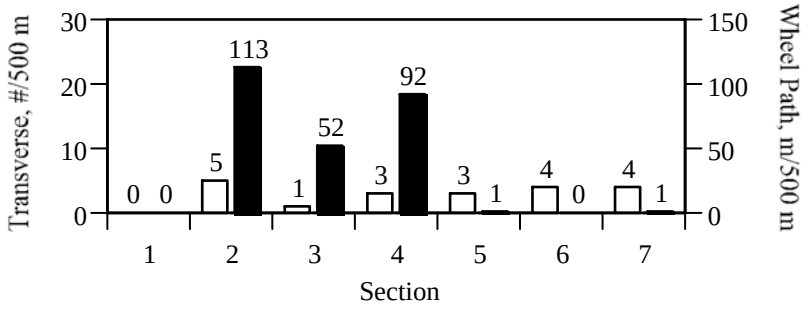

Figure 5. Summer 2006 Crack Survey
Note: Open bars for transverse cracking and solid bars for wheel path cracking.

Construction and Falling Weight Deflectometer Analysis

The first issue considered in analysing the distress data was whether the severe cracking in sections 2-4 was in some way related to variations in construction quality and subgrade consistency. Such variation is inevitable with pavement trials of this magnitude and with so many different types of asphalt binders.

Table 4 provides various properties assessed as possible confounding factors in the analysis of the pavement distress. These results were obtained as part of the end result specification (ERS) program in place for this contract and by which the pay factor was calculated.

TABLE 4. End Result Specification Findings

Section	AC, %	Voids, %		Pavement Thickness, mm
		Plate	In Situ	
1	4.81	5.6*	7.7	92.0
2	4.95	4.6	7.6	88.7
3	4.85	4.3	7.1	86.3
4	4.80	4.7	6.3	86.3
5	4.92	4.3	7.6	91.0
6	4.85	4.0	6.2	85.4
7	4.82	4.3	5.5	98.7
AVE ± SD	4.9 ± 0.1	4.5 ± 0.5	6.9 ± 0.9	89.8 ± 4.7

Note: All values were obtained as averages from three loose mix samples (plate) or cores (in situ) taken during and after construction of the trial. * This lot was rejectable based on the standard deviation, even though all three plate samples were acceptable within the limits.

It is obvious from the table that there was little variation in any of the properties commonly associated with wheel path cracking. Binder contents varied by no more than 0.1 percent, although they were consistently about 0.3 percent below the design of 5.2 percent. The voids as determined from compaction of loose mix taken during the paving operation were all, except for one, within a range of 0.7 percent, and the in situ voids measured from three cores were within a respectable range of 2.2 percent. The only section that may have benefited somewhat from lower voids was made with the control PG 52-34, which was obviously easier to

compact. Section 6 may become the only one to suffer due to a low thickness.

The next issue considered was the pavement stiffness variation within the site. Detailed falling weight deflectometer (FWD) testing was done during July 2005 (*28*). Measurements were taken in the northbound lane, in both the wheel path and mid-lane, every 20 metres throughout the monitoring portions of each section. In addition to the FWD testing, two boreholes per test section were advanced through the shoulder to a depth of 3 metres. The depths of the granular base, subbase, and subgrade as well as the water table were measured. Samples were taken for subsequent moisture determination. The borehole analysis showed that the site had a consistent structure with only section 6 having a lower base thickness and overall stiffness (*28*).

The detailed FWD data as presented in figure 6 show that, the site is fairly homogeneous within one standard deviation of the section's mean. There appears to be no relationship between pavement stiffness and the observed distress. However, it should be recognized that the FWD testing was done in July 2005, while most of the distress occurred from March to April of 2004. Hence, the subgrade consistency may have been somewhat different at the time of testing.

Section 1, with the lowest stiffness, has so far been free of cracking. Section 7 has somewhat of an advantage, due to the lower voids and higher thickness. Otherwise, the five remaining sections have nearly identical stiffness profiles. Hence, large differences in performance between these sections are likely due to material properties rather than design and construction differences.

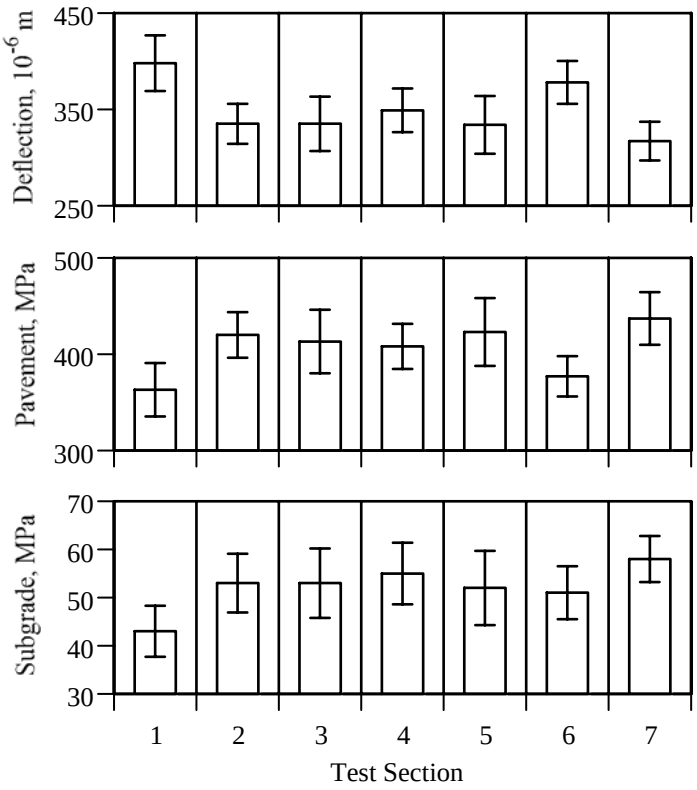

Figure 6. Falling Weight Deflectometer Data (July 2005)
Note: Each value is the average of 24 measurements around the monitoring portions of each section. Error bars provide ± 1 standard deviation of the mean.

Asphalt Binder Test Results

Dynamic Shear and Bending Beam Rheometer Testing

The Superpave® grades were strictly controlled at –34ºC, since this pavement trial was designed to assist in the development of an improved low temperature binder specification. Section 7 employed a PG 52-34 control that was used in the remainder of the contract; section 6 employed an oxidized PG 58-34; and the five remaining sections were made with PG 64-34 grades. With these grades came slight variations in the limiting fatigue temperature where G*sinδ reaches 5 MPa ranging from 6.7 to 10.1ºC.

However, close scrutiny of the data in table 1 shows that the Superpave® grading is unable to explain the distress as found in the test sections. Sections 1, 2, and 5 have nearly identical low temperature grades and loss moduli, yet one cracked severely and

the others did not. The binder used in section 3 has a somewhat lower loss modulus, yet it cracked quite severely.

In addition to the regular Superpave® grading, additional rheological testing was carried out to determine the complex modulus and phase angle master curves (figures 7 and 8) as well as Black space diagrams (figure 9). However, none of these investigations yielded any further insights to explain the performance differences observed in the field.

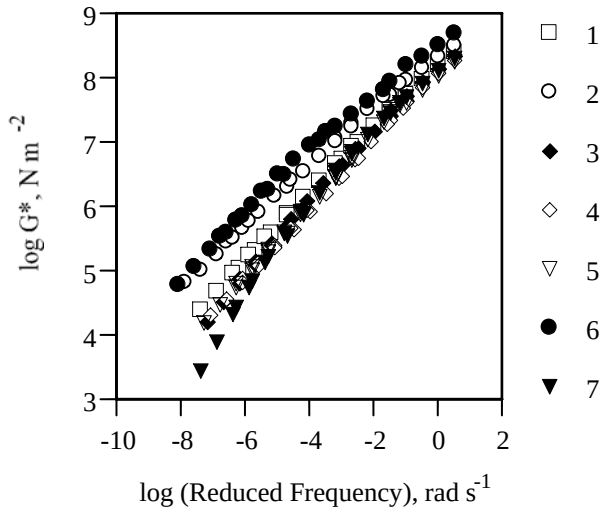

Figure 7. Complex Modulus Master Curves

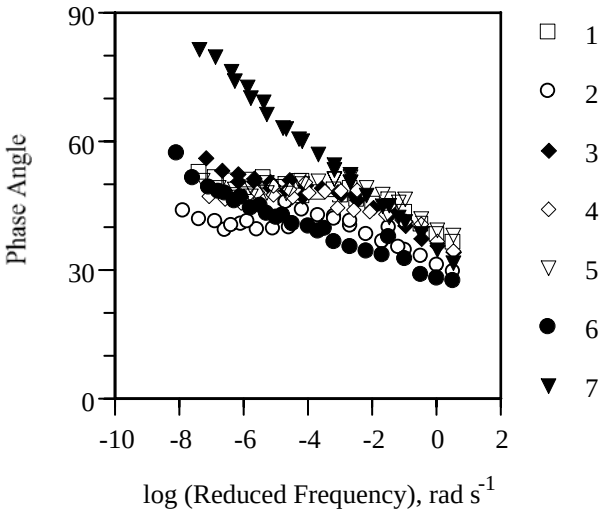

Figure 8. Phase Angle Master Curves

The Black space diagrams were unremarkable in that all binders except the one from section 7 showed moderate degrees of thermo-rheologically complex behaviour. Figure 9 provides the results for the binders from section 4 with the most complex behaviour together with section 7 with the least complex behaviour.

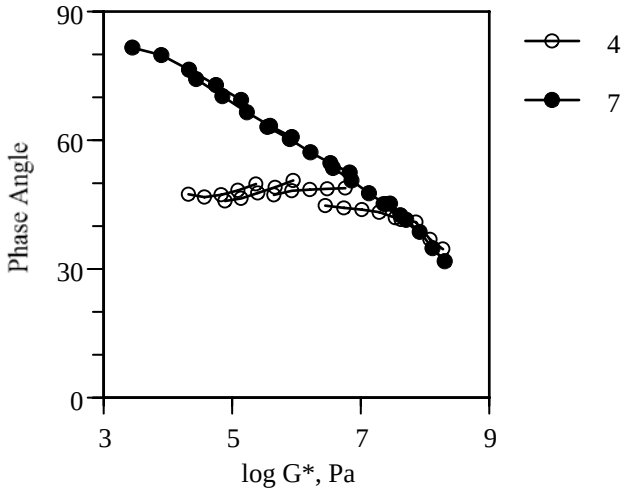

Figure 9. Black Space Diagram for Binders 4 and 7

In addition to the DSR testing, a significant amount of bending beam rheometer (BBR) testing was done according to Ontario's newly developed extended BBR method (*1, 6*). Figure 10 provides the grades for the seven binders as determined from tests on samples that were stored for three days at various conditioning temperatures. The results show that the binder used in section 2 suffered the most from reversible aging, while the binder used in section 1 suffered the least. However, the reversible aging effect does not entirely explain the distress. The binders used in sections 6 and 7 hardened by a considerable amount, yet they show very little cracking to date. The binder in section 3 hardened by a moderate amount, yet it exhibits extensive cracking. There must therefore be other differences between these binders that can explain the observed performance variation.

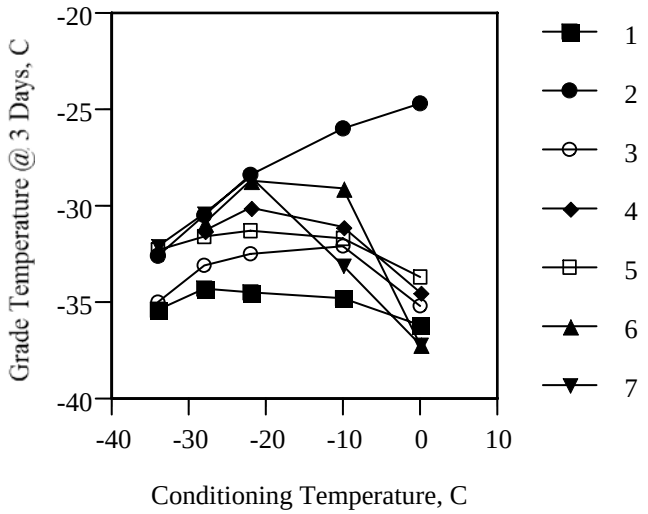

Figure 10. Extended Bending Beam Rheometer Results (*6*)
Note: Binders were stored for three days at the indicated storage temperatures. All binders graded under regular Superpave® protocols as PG XX-34.

Viscosity and Penetration Grading

The penetration and viscosity grading was done on unaged binders at Imperial Oil in Sarnia, Ontario. The results are provided in table 2. The data show that neither the viscosity or penetration values are able to explain the observed differences between the sections varying performance.

Double-Edge-Notched Tension Testing

Double-edge-notched tension tests were conducted on numerous specimens at different temperatures and rates of loading. The essential and plastic works of fracture were shifted along the logarithmic rate axis in order to form smooth master curves. Figure 11 shows the results of these tests for sections 1 and 2 (other binders showed similar results). Figure 12 shows the intercepts of all master curves representing the essential work of fracture (w_e, kJ m^{-2}) and plastic work terms (βw_p, MJ m^{-3}) at a 1 mm/min loading rate and 0ºC. It should be noted that the slopes of the failure energy master curves were all similar.

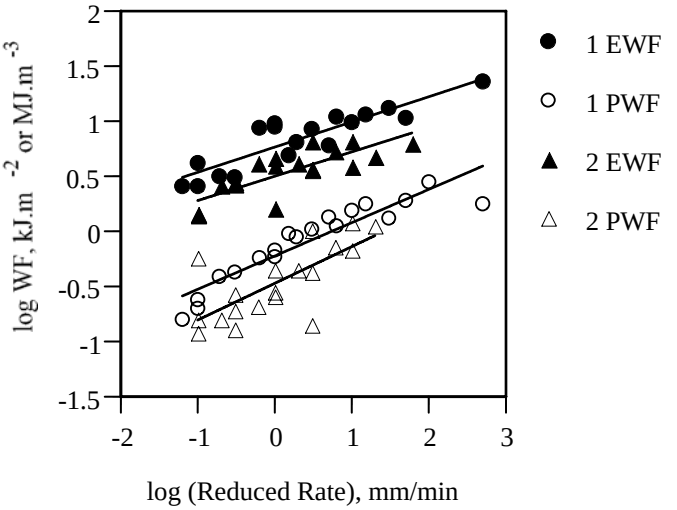

Figure 11. Failure Energy Master Curves
Note: Data were shifted to 0ºC to form smooth fracture energy master curves (*7*). Representative curves for binders 1 and 2 are given, while other binders showed similar results.

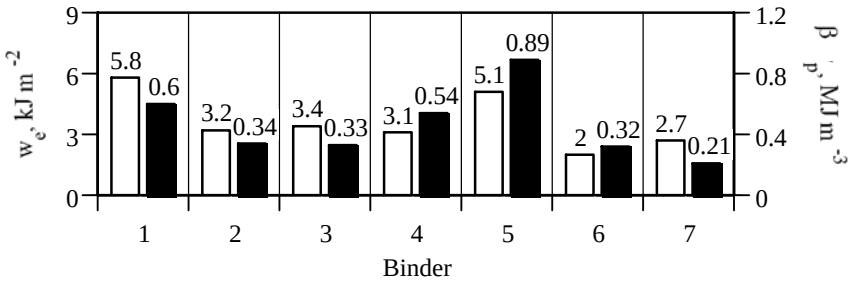

Figure 12. Essential and Plastic Work of Fracture Terms Under Standard Conditions (0ºC and 1 mm/min)
Note: Open bars for essential works of fracture and solid bars for plastic works of fracture.

It is clear from the data in figure 12 that a failure energy analysis alone is only able to partially explain the pavement distress. Sections 1 and 5 have sustained almost no damage thus far, and this could be explained by their high essential and plastic works of fracture. However, sections 6 and 7 have also performed well, while this figure shows them to possess the lowest ductile failure properties. Sections 2-4 have sustained various degrees of distress, yet show similar failure energies. Hence, there are obviously other factors that must be taken into consideration. One

parameter that has not yet been considered is the critical crack tip opening displacement, which is a property that provides a measure of strain tolerance in the presence of a crack in or near the ductile state (*4, 36*).

Figure 13 shows the critical crack tip opening displacement, δ_t, as approximated by the ratio of the essential work of fracture divided by the net section stress in the smallest ligament specimen, $\delta_t = w_e/\sigma_{net,\ 5\ mm}$. This property has been used extensively in the design of materials against failure at or near their ductile state and has been used by the authors to correctly rank the performance of the binders in the most recent FHWA ALF experiment (*4, 7, 38*).

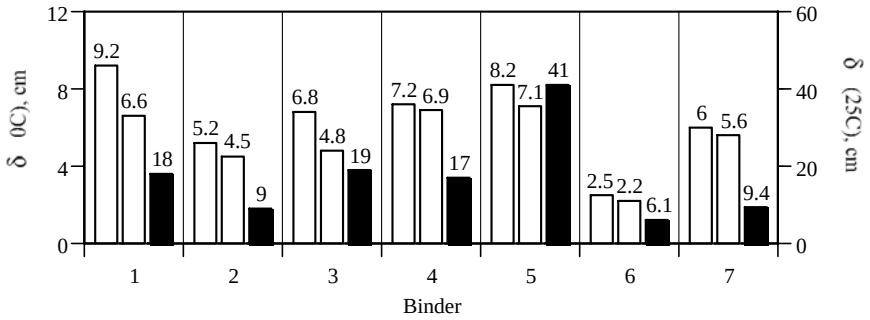

Figure 13. Binder Critical Crack Opening Displacements
Note: Open bars for 0ºC, 1 and 10 mm/min, respectively, and solid bars for 25ºC and 100 mm/min.

It is clear from these results that the binder tests alone will likely only provide a limited explanation for the observed distress. However, it is still reasonable to expect the long-term performance to be predicted by the data in figures 10, 12 and 13. Permanent deformation during summer months will likely aggravate the fatigue distress and hence sections 6 and 7 will perform worse in the long term due to their softer grades.

Asphalt Mixture Test Results

Complex Modulus and Phase Angle in Dynamic Compression

The complex modulus (figure 14) and phase angle (figure 15) master curves in dynamic compression were determined according to standard procedures as described in the experimental section.

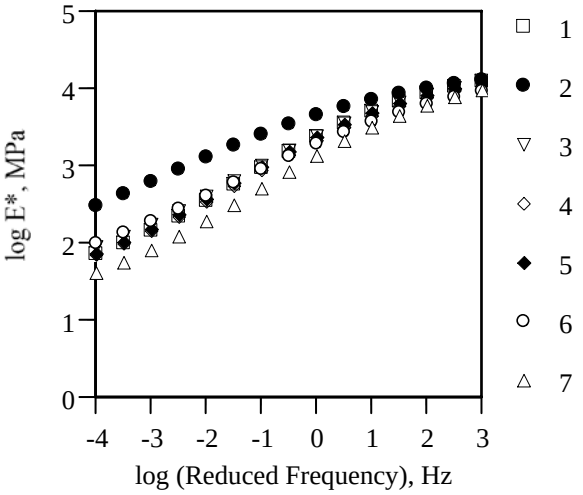

Figure 14. Dynamic Modulus Master Curves in Compression

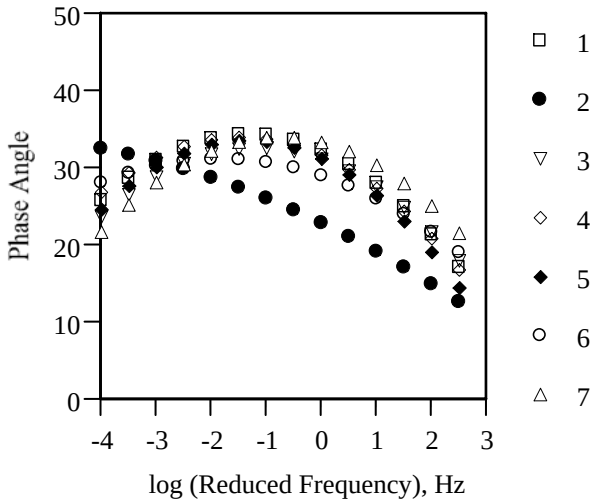

Figure 15. Phase Angle Master Curves in Compression

The results were largely unremarkable except for the tests on mixture 2 which showed both a significantly higher complex modulus and lower phase angle at all frequencies investigated. It is unclear at this moment what if any significance this has with respect to field performance since the other systems were all very similar yet showed very different performance in service. Mixtures 1 and 3-6 have nearly identical master curves while two are cracked severely and three are almost without any cracks.

These results show that the dynamic modulus and phase angle have limited use on their own for the prediction of asphalt performance in terms of the type of wheel path distress observed in this trial. The low strain properties as measured in the dynamic modulus protocol do not relate well with the high strain fracture behaviour of the mixtures when they were subjected to critical stresses during the 2004 cold spell and subsequent spring thaw.

Dynamic Fatigue in Four-Point Bending

Both the displacement- and force-controlled tests were conducted at room temperature, 25 ± 1ºC, a loading frequency of 10 Hz, and by using haversine pulses. The displacement-controlled tests were done at 600 micro strain, which rendered failure for all mixtures within a reasonable time. Since these tests typically take a long time, only one strain level was investigated thus limiting the information that can be obtained from the data.

The following failure criteria were included: (1) a 50 percent stiffness reduction; (2) a change in dissipated energy ratio (*32*); (3) a peak in the plot of (stiffness × number of cycles) versus number of cycles (*33*); and (4) a change in slope of the two-stage Weibull plot (*34*). The average number of cycles to failure for each mixture is given in figure 16, in the above order for each criterion.

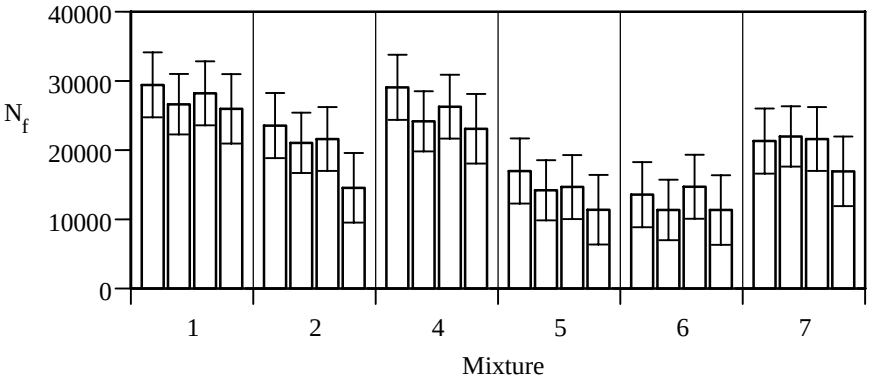

Figure 16. Number of Cycles to Failure in Displacement-Controlled Tests at 600 μm/m

Note: Mixture 3 was not tested due to materials and time limitations. Averages of between two and three samples are provided for each mixture. First bar provides failure according to a 50 percent stiffness reduction criterion; second bar according to the dissipated energy ratio; third bar according to the peak in stiffness × number of cycles plot; and fourth bar for change of slope in two-stage Weibull plot. Error bars provide ± one pooled standard deviation of the mean.

The data shows that a change in the failure criterion does not make a significant difference in the ranking for any of the mixtures. Only two mixtures, with very similar failure numbers, rank differently in the 50 percent stiffness reduction (first bar) compared to all the other rankings, which are consistent with each other. Further, there is no relationship between the endurance limits in this test and the field performance. Mixtures 5 and 6 rank last while in the field they have yet to show significant cracking. Mixture 4 ranks second best in figure 16 while the field performance is worst. Hence, it can be concluded that the controlled-displacement test is unable to predict the relative field performance for these mixtures. The reason for this failure is not entirely clear but may be related to differences between test and field in terms of loading mode, loading rate, stress state, and degree of stress concentration.

Using a 90 percent stiffness reduction failure criterion, the Wöhler curves for the force-controlled four-point bending tests are provided in figure 17. The data shows that the softer systems fail faster, which is as expected for a force-controlled test. However, once more there is no direct relation with the performance in the field (figures 4 and 5).

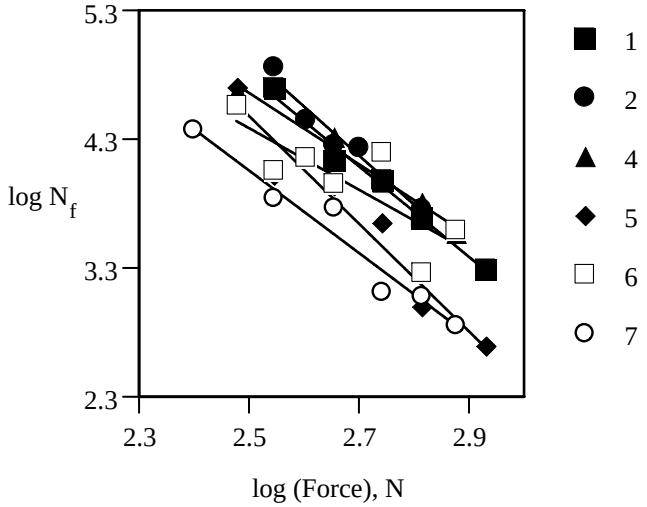

Figure 17. Wöhler Curves for Force Control
Note: Number of cycles to failure was determined at a 90 percent stiffness reduction. Mixture 3 was not tested due to materials and time limitations.

The load-controlled test data were also analysed according to the same failure criteria as listed above and once more the findings were not significantly altered by switching to a different definition of failure.

It is difficult to conceive that with heavy trucks driving over the pavement the loading can be anything else than a constant force situation. However, the stress state may be complex with a change from compressive to tensile components depending on the location relative to the position right underneath the tire. Further, the critical area where cracking initiates may be highly localized, making the situation more difficult to reproduce in a four-point bending experiment. For the relatively thin pavement used on Highway 655 the displacement reaches a certain level that depends on the composite pavement stiffness. Whether surface cracks appear will likely depend on the displacement, and hence the load applied and the pavement stiffness, but also on the strain tolerance of the materials. In order to draw meaningful conclusions from the four-point bending data, it may be necessary to involve a more sophisticated structural, mechanics, and energy analysis. However, this type of model development was beyond the scope of this work.

Dynamic Creep Fracture in Compact Tension

The dynamic creep fracture tests were conducted in compact tension with continuous 0.1 s haversine load pulses of 150 N. All tests were done at room temperature, 25 ± 1ºC. The number of load pulses was recorded at regular crack length intervals, and the data were fitted to an exponential. The exponential was numerically differentiated to obtain a smoothed crack growth rate, which was subsequently plotted versus the stress intensity factor, K_I, on a logarithmic scale. The results for all tests are given in figure 18.

The data shows that for all mixtures except the mixture representing section 2 there is a large degree of scatter which is similar to what is reported by others (*39*). The scatter can be attributed to the fact that this test was done on relatively small samples for a 12.5 mm maximum aggregate size. Moreover, the nature of dynamic crack growth tests is such that large degrees of scatter are unavoidable.

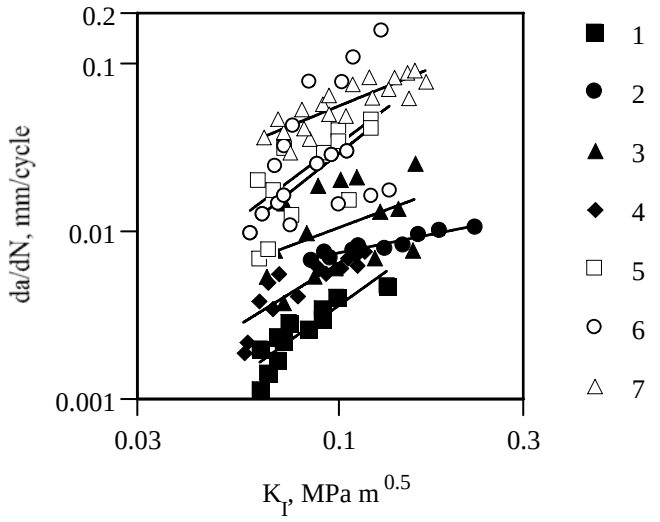

Figure 18. Dynamic Creep Crack Growth in Compact Tension

The relative rankings show somewhat expected trends similar to the load-controlled four-point bend results in that the softer systems (mixtures 7, 6, and 5) respond with high rates of crack growth compared to the stiffer systems (mixtures 1, 2, and 4). However, there appears to be no simple relationship between the rate of crack growth and the cracking severity in the field (figures 4 and 5). In order to draw meaningful conclusions from this data, it may be necessary to involve a more sophisticated structural analysis. Furthermore, additional measurements of crack tip opening displacement in the fatigue test would be helpful to differentiate between good and not so good systems. However, such measurements are either difficult to perform or would involve a number of assumptions. Hence, our efforts have considered the essential work of fracture approach that provides measures of critical failure properties that are more easily obtained.

Double-Edge-Notched Tension

The DENT tests provide a measure of the essential and plastic works of fracture, w_e and βw_p, as well as an approximation of the critical crack opening displacement from the ratio of w_e over the net section stress of the smallest ligament specimen, $\delta_t = w_e/\sigma_{net}$.

Samples were all tested at 25 ± 1ºC and 5.4 mm/min, which guaranteed ductile failure in all systems. For most tests the reproducibility was found to be good although not as good as for

the binder tests. The only exception was for the mixture representing section 4, which showed a somewhat higher variability. The force versus displacement curves were all found to be self-similar for different ligament lengths (i.e., were similarly shaped), and the data fit equation 1 with reasonable accuracy, thus providing some degree of validity to the essential work of fracture approach.

Representative results for the analysis according to equation 1 are given for mixtures 1, 5, and 7 in figure 19, while typical net section stresses as a function of ligament length are given for mixtures 3, 5, and 7 in figure 20. Other mixtures gave similar results. The data are interesting in several respects. First, the specific total works of fracture vary by a substantial amount between mixtures, although the scatter is larger than in the binder tests. Second, the net section stress for mixture 3 is significantly higher than that of mixtures 5 and 7. This causes the mixture to be less strain tolerant and explains to some degree the fact that section 3 was severely cracked after just the first winter. The same high net section stresses were found for mixtures 2 and 4, thus providing a simple explanation of why these performed so poorly in the field.

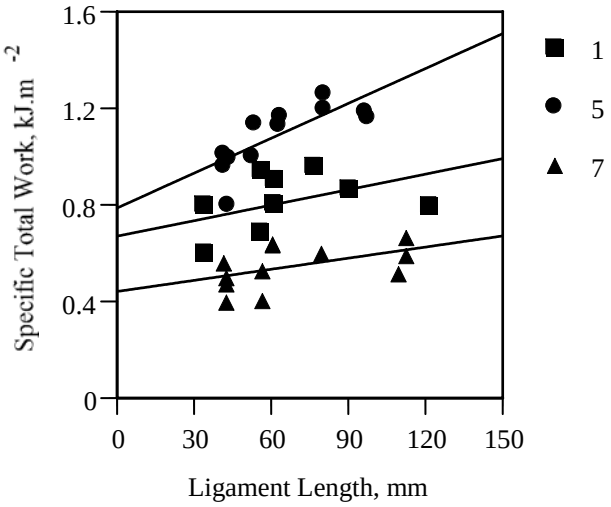

Figure 19. Essential Works of Fracture for Mixtures 1, 5, and 7
Note: Other systems gave similar results.

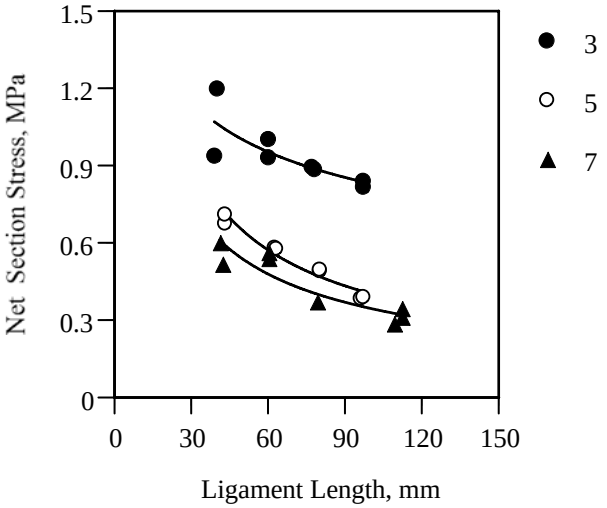

Figure 20. Net Section Stresses as Function of Ligament Length for Mixtures 3, 5, and 7
Note: Other systems gave similar results. Only mixture 4 gave somewhat higher variability.

The critical crack opening displacement was approximated by dividing the essential work of fracture by the net section stress in the smallest ligament length. The results for w_e and δ_t for all mixtures are given in figure 21.

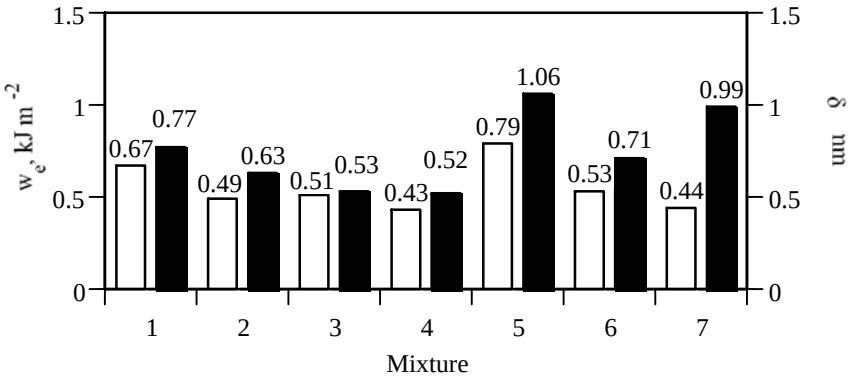

Figure 21. Essential Works of Fracture and Approximate Critical Crack Opening Displacements for Mixtures 1-7
Note: Open bars for essential works of fracture and solid bars for critical crack opening displacement.

The results in figure 21 are in general agreement with the severity of distresses noted within the trial sections. Sections 2-4 have the lowest critical crack opening displacements and are the most severely cracked. Sections 1 and 5-7 have the highest critical crack opening displacements and have performed very well without showing signs of early distress.

The fact that section 2 has cracked more than section 3 can likely be explained by the fact that binder 2 reversibly ages much more (figure 10), which would have initiated more micro cracks during the excursions at low temperatures. Moreover, binder 3 reversibly ages less than binder 4, and appears to be of lower viscosity, and thus will heal cracks more readily during summer months, which could in part explain the lower amount of distress.

The future will likely show that sections 1 and 5 outperform sections 6 and 7, since they have significantly higher essential works of fracture and high temperature performance grades. In long-life pavements the rutting distress will undoubtedly feed the surface initiated cracking, making the picture more complex than what it appears after just three years of service.

It is interesting to note that sections 3-5 were all made with SBS-modified materials but the amount of polymer in sections 3 and 4 must have been much less than that used in section 5. The performance of this trial shows that not all PG 64-34 grades perform the same and that the use of acid and other non-polymer (chemical) modifiers may lead to premature cracking in service (*40*).

SUMMARY AND CONCLUSIONS

Given the review of the literature and the results presented in this paper, the following summary and conclusions are provided:

- The binder loss modulus, G*sinδ, provides only a crude measure of fatigue performance and is not able to correctly rank the Highway 655 materials. This conclusion agrees with the findings of our earlier study of FHWA ALF materials (*4*).
- Binders with approximately equal works of fracture but with different yield stresses will likely show differences in

fatigue, with the lower yield stress material outperforming the higher yield stress material. Hence, binder or mixture fracture energy alone will likely only be able to rank materials with similar yield stresses in pure fatigue.

- Since crack tip opening displacement, δ_t, provides a measure of strain tolerance in the presence of sharp cracks in the ductile-to-brittle and fully ductile states, it provides an ideal parameter to grade asphalt binders, mastics, and mixtures for pure fatigue distress.
- Long-term performance may correlate better with the essential work of fracture since it captures the effects of both pure fatigue at ambient temperatures and rutting at higher temperatures.
- The asphalt-aggregate interface is nonexistent in binder tests hence such tests may not be able to provide a complete assessment of fatigue resistance in the field. Asphalt mastic and mixture tests will likely succeed when binder tests alone are inconclusive.
- Complex modulus and phase angle master curves, four-point bending fatigue, and compact tension fatigue tests on mixtures showed poor correlations with field performance.
- Monotonic DENT tests correlated reasonably well with field distress. However, the DENT data needed to be supplemented with reversible aging tendencies to provide a complete interpretation of the distress variation within the trial.

FURTHER WORK

It will be worthwhile to further follow the performance of the seven test sections. Likely the long term performance will be confounded with the different degrees to which the base asphalts and modifiers age, due to the combined effects of volatilization, oxidation, and moisture damage. However, all of these factors can be assessed by taking core samples from the road to allow testing of the extracted binders (*6*).

The use of falling weight deflectometer testing in both lanes in years to come will also be helpful to delineate between load and moisture induced distress.

Priority should be given to develop an asphalt mastic test based on the essential work of fracture approach to see if it can bridge the gap between the data in figures 4 and 5 (field cracking severity) and figures 12 and 13 (binder failure properties). Such test would save a considerable amount of time and equipment cost by eliminating the need for mixture testing (figure 21).

Evaluation of this pavement trial shows that with reasonable time, effort, and expenditure, significant progress can be made for future pavement performance by including the findings in new specifications.

ACKNOWLEDGMENTS

The authors would like to thank Dale Smith of the Northeastern Regional Office of the Ontario Ministry of Transportation for obtaining the falling weight deflectometer data. Staff of the Bituminous Section at the Ontario Ministry of Transportation are thanked for sample preparation and instruction on the four-point bending fatigue test.

Irsan Kodrat of Queen's University is thanked for his assistance in obtaining essential work of fracture results at 0ºC.

Additional recognition goes to Lyle Moran and Mary Gale of Imperial Oil, who helped with securing the PAV-aged asphalt binders and grading information used in this study.

Nelson Gibson of FHWA is thanked for facilitating the E* and simple performance testing for the Highway 655 mixtures and for providing the test method description. Frank Davis and Scott Parobeck of FHWA/SaLUT Inc., provided the test data, and Ghazi Al-Katheeb of FHWA/SaLUT Inc., processed the data.

Appreciation is expressed to Maureen Garvie of Kingston, Ontario, and Pamela Marks of the Ontario Ministry of Transportation in Downsview, Ontario, for the proof-reading of this manuscript.

The authors are grateful for the financial support provided by the Charitable Foundation of Imperial Oil Limited, the Innovations Deserving Exploratory Analysis Program (IDEA) as administered by the National Cooperative Highway Research Program, the Ontario Ministry of Transportation, and by the Natural Sciences and Engineering Research Council of Canada.

DISCLAIMER

None of the sponsoring agencies necessarily concurs with, endorses, or has adopted the findings, conclusions or recommendations either inferred or expressly stated in subject data developed in this study.

References

(1) Ministry of Transportation of Ontario. *LS-308 – Method of Test for Determination of Performance Grade of Physically Aged Asphalt Cement Using Extended Bending Beam Rheometer (BBR) Method.* Revision 23 to MTO Laboratory Testing Manual, February 2006.

(2) Andriescu, A., S.A.M. Hesp, J.S. Youtcheff. "Essential and Plastic Works of Ductile Fracture in Asphalt Binders." *Journal of the Transportation Research Board, Transportation Research Record,* No. 1875, 2004, pp. 1-8.

(3) Andriescu, A., S. Iliuta, S.A.M. Hesp, J.S. Youtcheff. "Essential and Plastic Works of Ductile Fracture in Asphalt Binders and Mixtures." *Proceedings, Canadian Technical Asphalt Association,* Vol. 49, 2004, pp. 93-121.

(4) Andriescu, A., N.H. Gibson, S.A.M. Hesp, X. Qi, and J.S. Youtcheff. "Validation of the Essential Work of Fracture Approach to Fatigue Grading of Asphalt Binders." *Journal of the Association of Asphalt Paving Technologists,* Vol. 75E, 2006, pp. 1-37.

(5) Ministry of Transportation of Ontario. *LS-299 (Draft) – Method of Test for Asphalt Cement's Resistance to Fatigue Fracture Using Double-Edge-Notched Tension Test (DENT).* Revision 23 to MTO Laboratory Testing Manual, February 2006.

(6) Iliuta, S., A. Andriescu, S.A.M. Hesp, and K.K. Tam. "Improved Approach to Low-Temperature and Fatigue Fracture Performance Grading of Asphalt Cements." *Proceedings, Canadian Technical Asphalt Association*, Vol. 49, 2004, pp. 123-158.

(7) Andriescu, A. *Essential Work of Fracture Approach to Fatigue Grading of Asphalt Binders.* Doctoral Dissertation, Queen's University, Kingston, Ontario, August 2006.
(8) Pell, P.S. "Fatigue Characteristics of Bitumen and Bituminous Mixes." *Proceedings, International Conference on Structural Design of Asphalt Pavements,* Ann Arbor, Michigan, U.S.A., August 20-24, 1962.
(9) *Fatigue Response of Asphalt-Aggregate Mixes.* SHRP-A-404 Final Report. Strategic Highway Research Program, National Research Council, Washington D.C., 1994.
(10) Van Dijk, W. "Practical Fatigue Characterization of Bituminous Mixes." *Proceedings, Association of Asphalt Paving Technologists,* Vol. 44, 1975, pp. 38-74.
(11) Van Dijk, W., and W. Visser. "The Energy Approach to Fatigue for Pavement Design." *Proceedings, Association of Asphalt Paving Technologists,* Vol. 46, 1977, pp. 1-40.
(12) Aglan, H., A. Othman, and L. Figueroa. "The Specific Energy of Damage as a Fracture Criterion for Asphaltic Pavements." *Journal of the Transportation Research Board, Transportation Research Record,* No. 1449, 1994, pp. 57-63.
(13) Kim, Y.R., H.-J. Lee, and D.N. Little. "Fatigue Characterization of Asphalt Concrete Using Viscoelasticity and Continuum Damage Theory." *Journal of the Association of Asphalt Paving Technologists,* Vol. 66, 1997, pp. 520-569.
(14) Daniel, J.S., W. Bisirri, and Y.R. Kim. "Fatigue Evaluation of Asphalt Mixtures Using Dissipated Energy and Continuum Damage Approaches." *Journal of the Association of Asphalt Paving Technologists,* Vol. 73, 2004, pp. 557-584.
(15) Lundström, R., and U. Isacsson. "An Investigation of the Applicability of Schapery's Work Potential Model for Characterization of Asphalt Fatigue Behavior." *Journal of the Association of Asphalt Paving Technologists,* Vol. 73, 2004, pp. 657-695.
(16) Uzan J., F. Zhou, and R.L. Lytton. "Fracture Energy: What Is It in a Visco-Elastic Visco-Plastic Material?" *Journal of the Association of Asphalt Paving Technologists,* Vol. 74E, 2005, pp. 1-27.
(17) Roque, R., B. Birgisson, B. Sangpetgnam, Z. Zhang. "Crack Growth Behavior of Asphalt Mixtures and Its Relation to Laboratory and Field Performance." *Proceedings, 8th*

International Conference on Asphalt Pavements, Copenhagen, Denmark, 2002.
(18) Meyers, L.A., and R. Roque. "Top-Down Crack Propagation in Bituminous Pavements and Implications for Pavement Management." *Journal of the Association of Asphalt Paving Technologists,* Vol. 71, 2002, pp. 651-670.
(19) Zhang, Z., R. Roque, B. Birgisson, B. Sangpetgnam. "Identification and Verification of a Suitable Crack Growth Law for Asphalt Mixtures." *Journal of the Association of Asphalt Paving Technologists,* Vol. 70, 2001, pp. 206-241.
(20) Roque, R., B. Birgisson, C. Drakos, and B. Dietrich. "Development and Field Evaluation of Energy-Based Criteria for Top-Down Cracking Performance of Hot Mix Asphalt." *Journal of the Association of Asphalt Paving Technologists,* Vol. 73, 2004, pp. 229-260.
(21) Cotterell, B., and J.K. Reddel. "The Essential Work of Plane Stress Ductile Fracture." *International Journal of Fracture*, Vol. 13(3), 1977, pp. 267-277.
(22) Mai, Y.-W., S.-C. Wong, and X.-H. Chen. "Application of Fracture Mechanics for Characterization of Toughness of Polymer Blends." In: *Polymer Blends, Volume 2: Performance.* D.R. Paul and C.B. Bucknall (Eds.), Wiley and Sons, 2000.
(23) Ferne, B. "Long-Life Pavements–a European Study by ELLPAG." *International Journal of Pavement Engineering,* Vol. 7(2), 2006, pp. 91-100.
(24) Merrill, D., A. van Dommelen, and L. Gaspar. "A Review of Pratical Experience Throughout Europe on Deterioration in Fully-Flexible and Semi-Rigid Long-Life Pavements." *International Journal of Pavement Engineering,* Vol. 7(2), 2006, pp. 101-109.
(25) Wistuba, M., R. Lackner, R. Blab, and M. Spiegl. "Low-Temperature Performance Prediction of Asphalt Mixtures Used for LLP–New Approach Based on Fundamental Test Methods and Numerical Modeling." *International Journal of Pavement Engineering,* Vol. 7(2), 2006, pp. 121-132.
(26) Yee, P., B. Aida, S.A.M. Hesp, P. Marks, and K.K. Tam. "Analysis of Three Premature Low Temperature Pavement Failures." *Journal of the Transportation Research Board,* In Press, July 2006.

(27) LTPPBIND® Software, Version 2.1, Federal Highway Administration, McLean, Virginia, 1999.
(28) *Falling Weight Deflectometer Testing and Soil Investigation. Seven Pavement Test Sections – Highway 655.* Thunder Bay Testing and Engineering Limited, July 27, 2005.
(29) AASHTO TP62-03, "Determining Dynamic Modulus of Hot Mix Asphalt Concrete Mixtures." *2005 AASHTO Provisional Standards*, Eighth Edition, American Association of State Highway and Transportation Officials, Washington D.C., 2005.
(30) Witczak, M., K. Kaloush, T. Pellinen, M. El-Basyouny, and H.V. Quintus. *Simple Performance Test for Superpave® Mix Design.* NCHRP Report 465, National Research Council, Washington, D.C., 2002.
(31) Bonaquist, R.F, D.W. Christensen, and W. Stump. *Simple Performance Tester for Superpave® Mix Design: First-Article Development and Evaluation.* NCHRP Report 513, National Research Council, Washington, D.C., 2003.
(32) Pronk, A.C. *Evaluation of the Dissipated Energy Concept for the Interpretation of Fatigue Measurements in the Crack Initiation Phase.* Report No. P-DWW-95-501, Ministry of Transportation, The Netherlands.
(33) Rowe, G.M., and M.G. Bouldin. "Improved Techniques to Evaluate Fatigue Resistance of Asphaltic Mixtures." *Proceedings, Eurasphalt & Eurobitume Congress,* Barcelona, Spain, September 2000, Book 1, pp. 754-763.
(34) Tsai, B.-W., T.J. Harvey, and C.L. Monismith. "Two-Stage Weibull Approach for Asphalt Concrete Fatigue Performance Prediction." *Journal of the Association of Asphalt Paving Technologists,* Vol. 71, 2002, pp. 365-407.
(35) Zuidema, J., A.C. Pronk, and F. Tolman. "Fatigue and Creep Crack Growth in Asphalt Materials." Progress in Mechanical Behaviour of Materials, *Proceedings of the International Conference on the Mechanical Behaviour of Materials,* 8th, Victoria, BC, Canada, May 16-21, 1999 (1999), 1 424-428.
(36) Pronk, A., and S. Erkens. "A Note on Fatigue Bending Tests Using Haversine Loading." *Road Materials and Pavement Design,* Vol. 3(1), 2002, pp. 95-106.
(37) McCrum, N.G., C.P. Buckley, and C.B. Bucknall. *Principles of Polymer Engineering.* Oxford Science Publications, 1995.

(38) Roy, S.D., and S.A.M. Hesp. “Fracture Energy and Critical Crack Tip Opening Displacement.” *Proceedings, Canadian Technical Asphalt Association*, Vol. 46, 2001, pp. 187-214.
(39) Collop, A.C., A.J. Sewel, and N.H. Thom. “Assessment of the Resistance to Crack Propagation in Asphaltic Materials Using the Compact Tension Test.” *Proceedings, Fifth International RILEM Conference on Cracking in Pavements*, Limoges, France, May 5-8, 2004, pp. 691-698.
(40) Kodrat, I., D. Sohn, and S.A.M. Hesp. “How Polyphosphoric Acid-Modified Asphalt Binders Compare with Straight and Polymer-Modified Materials.” Pre-Print Paper No. 07-0949, 86th Annual Meeting, Transportation Research Board, Washington, D.C., January 2007.